

- [23] Sivanathan, S., Kirubarajan, T., and Bar-Shalom, Y. (1999) A radar power multiplier algorithm for acquisition of low observable ballistic missiles using an electronically scanned array radar. *IEEE Transactions on Aerospace and Electronic Systems*, 37, 1 (April 2001), 401–418.
- [24] Sworder, D. D., and Hutchins, R. G. (1989) Image-enhanced tracking. *IEEE Transactions on Aerospace and Electronic Systems*, 25, 5 (Sept. 1989), 701–710.
- [25] Sworder, D. D., Hutchins, R. G., and Kent, M. (1993) Utility of imaging sensors in tracking systems. *Automatica*, 29, 2 (Mar. 1993), 445–449.

## Multicarrier Radar Signal—Pulse Train and CW

A multicarrier complementary phase-coded (MCPC) radar signal employs  $N$  subcarriers *simultaneously*. The subcarriers are phase modulated by  $N$  different sequences that constitute a *complementary* set. The subcarriers are frequency-separated by the inverse of the duration of a phase element  $t_b$ . An  $N \times M$  MCPC pulse achieves pulse compression ratio of  $NM$ . When an  $N \times M$  MCPC signal is used in a coherent train of  $N$  pulses (e.g., in order to allow Doppler processing), it is advantageous to use pulse diversity. Each pulse is constructed using a different cyclic frequency shift of the first pulse. Such pulse diversity eliminates recurrent lobes at multiples of the pulse repetition interval. The constant volume property of the ambiguity function is maintained by shifting volume from the recurrent lobes to the sidelobe pedestal strips. However, if the sequence ordering along frequencies in the  $N$  pulses are arranged to create a complementary set in each frequency as well as in each pulse, the sidelobe level around the main autocorrelation lobe is dramatically reduced. Preferred MCPC coding for CW mode (contiguous MCPC pulses) and their delay-Doppler response are also discussed.

### I. INTRODUCTION

A multicarrier (or multifrequency) complementary phase-coded (MCPC) radar signal was described recently [1, 2]. An MCPC pulse employs  $N$  subcarriers *simultaneously*. The subcarriers are phase modulated by  $N$  different code sequences that together constitute an  $N \times M$  *complementary* set. A

Manuscript received September 2, 2000; revised March 15 and November 1, 2001 and February 11, 2002; released for publication February 22, 2002.

IEEE Log No. T-AES/38/2/11456.

Refereeing of this contribution was handled by L. M. Kaplan.

0018-9251/02/\$17.00 © 2002 IEEE

CORRESPONDENCE

square complementary set ( $M \times M$ ) can be easily constructed from the  $M$  cyclic shifts of an ideal phase-coded sequence of length  $M$ . (Ideal sequence has an ideal periodic autocorrelation function (ACF), e.g., P4, defined in (4)). Henceforth we deal mostly with  $M \times M$  MCPC pulses. The subcarriers are frequency-separated by the inverse of the duration of a phase element  $t_b$ , yielding orthogonal frequency division multiplexing (OFDM), well known in communications. A single  $N \times M$  MCPC pulse exhibits a thumbtack ambiguity function with delay resolution of  $t_b/N$  and Doppler resolution of  $1/(Mt_b)$ . The power spectrum is relatively flat with width of  $N/t_b$ . While the signal modulating each one of the subcarriers exhibits a fixed real-amplitude, the entire MCPC signal exhibits a variable real-amplitude. A single  $M \times M$  MCPC pulse, based on a specific complementary set of sequences, can be generated in  $M!$  different permutations. In each permutation the  $M$  sequences comprising the set are arranged in a different order along the  $M$  frequencies. With some permutations the peak-to-mean envelope power ratio (PMEPR) can be maintained below 2.

The present paper emphasizes the use of  $M \times M$  MCPC pulses in a coherent train of  $M$  pulses. Coherent pulse trains are required for Doppler processing, e.g., in MTI radar. In a coherent train of MCPC pulses, some additional advantages can be gained by introducing diversity between pulses, especially if each pulse is constructed using a different one of the  $M$  possible one-way cyclic frequency shifts of the first pulse. Such a construction ensures that a complementary set is found also when one looks at any single subcarrier in all the pulses. Note that there are  $M!$  possible permutations of ordering the  $M$  diverse pulses in time.

Using such pulse diversity does not degrade the ability to perform Doppler filtering. On the other hand it yields two important advantages. 1) It *totally* eliminates the recurrent ambiguity lobes at multiples of the pulse repetition interval. (The constant volume property of the ambiguity function is maintained by shifting volume from the recurrent lobes to the pedestal strips.) 2) The suggested diversity yields significant sidelobe reduction around the main autocorrelation lobe. This reduction is further enhanced when the diversity is combined with amplitude weighting of the different subcarriers. Henceforth, this type of weighting is referred to as “frequency weighting.”

### II. SINGLE MCPC PULSE

A schematic description of an  $M \times M$  MCPC pulse is given in Fig. 1. It shows  $M$  ( $= 5$ ) sequences modulating  $M$  subcarriers. Each sequence is constructed from  $M$  elements each of duration  $t_b$ . The total pulse duration is  $Mt_b$ . The autocorrelation

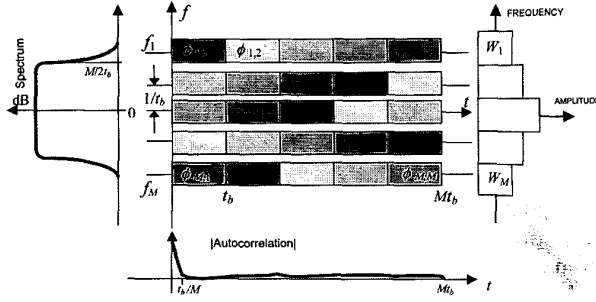


Fig. 1. Structure of  $M \times M$  MCPC pulse.

mainlobe width of such a signal is  $t_b/M$ . This mainlobe width is comparable to the mainlobe width of a single-frequency pulse-compression radar signal (e.g., P4) with  $M^2$  elements and the same overall pulse duration. We also show that the MCPC pulse exhibits an efficient spectrum usage. As depicted on the left-hand side (LHS) of Fig. 1, the power spectrum of the complex envelope is nearly rectangular with cutoff at  $f \approx M/(2t_b)$ . Frequency weighting, depicted on the right-hand side (RHS) of Fig. 1, modifies the spectrum.

The autocorrelation sidelobes will be lower if instead of repeating the same sequence on all frequencies, the sequences will be different, but will constitute a complementary set [3]. A complex valued sequence  $X_i$ , whose  $k$ th element is  $s_i(k)$ , forms a complementary set if the sum  $Z(p)$  of the aperiodic ACF  $R_i$  of all sequences from the set is equal to zero for all non-zero time shifts  $p$ , i.e.,

$$Z(p) = \sum_{i=0}^{M-1} \sum_{k=0}^{M-1-p} s_i(k) s_i^*(k+p) = \begin{cases} \sum_{i=0}^{M-1} R_i(0), & p = 0 \\ 0, & p \neq 0 \end{cases} \quad (1)$$

where  $*$  denotes complex conjugate,  $p$  is the (positive) time shift, and  $R_i(0)$  is the energy of the sequence  $X_i$ . A simple example: When the set has only two sequences (a complementary pair), the two sequences (of equal length  $M$ ) must have aperiodic ACFs whose sidelobes are equal in magnitude but opposite in sign. The sum of the two ACFs has a peak of  $2M$  and a sidelobe level of zero.

An  $M \times M$  complementary set can be constructed using Popovic's [4] result which states that *all the different cyclic time shifted versions of any sequence having an ideal periodic ACF, form a complementary set*. Useful polyphase code sequences that exhibit ideal periodic ACF are the P3 and P4 signals [5]. Useful two-phase code sequences with ideal periodic autocorrelation were suggested by Golomb [6]. Binary

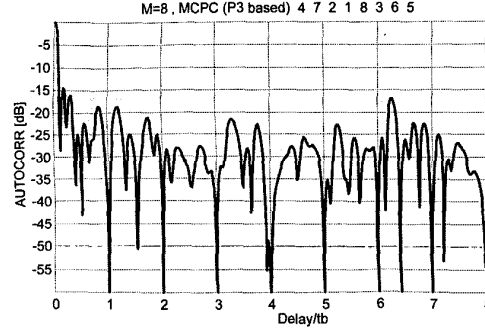


Fig. 2. Autocorrelation of  $8 \times 8$  MCPC pulse based on P3 sequence.

phase sequences (using  $0^\circ$  and  $180^\circ$ ) with ideal periodic autocorrelation are rare. Barker code of length 4 is an example. Other binary complementary sets can be constructed by methods other than cyclic shifts, e.g., from Hadamard matrices.

The mathematical expression of the complex envelope of an  $N \times M$  MCPC pulse is given by

$$u(t) = \begin{cases} \sum_{n=1}^N W_n \exp \left[ j2\pi \left( \frac{N+1}{2} - n \right) t/t_b \right] \\ \quad \times \sum_{m=1}^M u_{n,m}[t - (m-1)t_b], & 0 \leq t \leq Mt_b \\ 0, & \text{elsewhere} \end{cases} \quad (2)$$

where

$$u_{n,m}(t) = \begin{cases} \exp(j\phi_{n,m}), & 0 \leq t \leq t_b \\ 0, & \text{elsewhere} \end{cases} \quad (3)$$

$\phi_{n,m}$  is the  $m$ th phase element of the  $n$ th code sequence, and  $W_n$  is the amplitude weight assigned to the  $n$ th subcarrier.  $W_n$  can have a complex value, reflecting the option to control the polarity or phase of each subcarrier.

We first consider phase elements  $\phi_{n,m}$  of the  $M \times M$  matrix constructed from all the cyclic shifts of polyphase coded sequence [5] like a P4 code described by

$$\phi_m = \frac{\pi}{M}(m-1)^2 - \pi(m-1), \quad m = 1, 2, \dots, M \quad (4)$$

or a P3 (or Chu) code described by

$$\phi_m = \begin{cases} \frac{\pi}{M}(m-1)^2, & M \text{ even} \\ \frac{\pi}{M}(m-1)m, & M \text{ odd} \end{cases}, \quad m = 1, 2, \dots, M. \quad (5)$$

Note that the polydromic modification of the P4 signal [5] could not serve as a basis for an MCPC signal because its periodic ACF is not ideal.

TABLE I  
Phase Matrix [deg.] of  $8 \times 8$  MCPC Based on P3

0	22.5	90	202.5	0	202.5	90	22.5
22.5	90	202.5	0	202.5	90	22.5	0
90	202.5	0	202.5	90	22.5	0	22.5
202.5	0	202.5	90	22.5	0	22.5	90
0	202.5	90	22.5	0	22.5	90	202.5
202.5	90	22.5	0	22.5	90	202.5	0
90	22.5	0	22.5	90	202.5	0	202.5
22.5	0	22.5	90	202.5	0	202.5	90

For P3 and  $M = 8$ , the phase (modulo  $360^\circ$ ) matrix of all the cyclic shifts is given in Table I. (Note that the sequence on the fifth row from the top is a P4 sequence.) The set of complex elements with uniform magnitude, whose phase is described by Table I, will remain a complementary set for any reordering of the rows. When one particular order (stated on the illustrations) is used as  $\phi_{n,m}$  in (2) and (3), the resulting complex envelope will exhibit an ACF and power spectral density as depicted in Figs. 2 and 3, respectively. Note that it was also assumed that  $W_n = 1$  for all  $n$ . A multicarrier signal, as defined in (2) (i.e., weighted coherent sum of all the carriers), yields a typical autocorrelation function (ACF) as given in Fig. 2. The mainlobe extends as far as  $t_b/M$  with low sidelobes elsewhere. For comparison, in a single-carrier P3 or P4 signal with chip duration  $t_b$ , the ACF mainlobe will extend as far as  $t_b$ . Note also the complete nulls of the ACF at multiples of  $t_b$ . These nulls are inherent as long as  $W_n = 1$ . The particular ACF given in Fig. 2, was obtained for a signal based on the phase matrix of Table I, in which the order of rows underwent permutations according

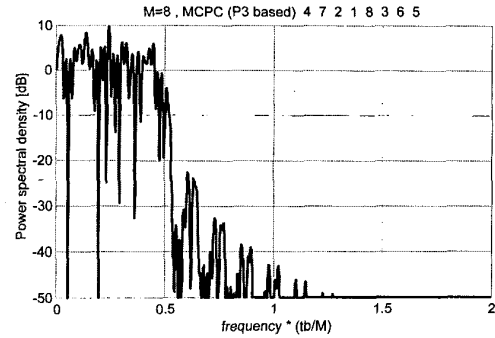


Fig. 3. Power spectrum of signal used in Fig. 2.

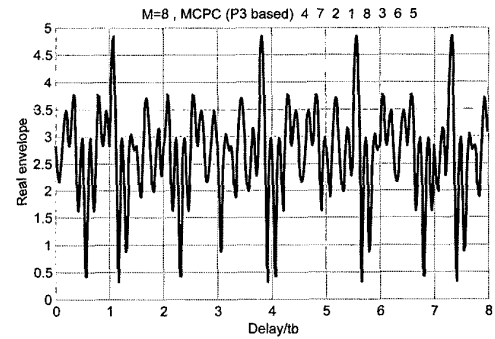


Fig. 4. Real envelope of signal used in Fig. 2.

to the list of eight numbers at the heading of Fig. 2. The heading indicates that the carrier at the highest frequency was phase modulated by the sequence in the fourth row (from the top) of Table I, and the lowest frequency carrier was phase modulated by the sequence in the fifth row.

Fig. 3 presents the spectrum of the complex envelope. Note a relatively flat spectrum extending from  $-M/2t_b$  to  $M/2t_b$  (negative half not plotted).

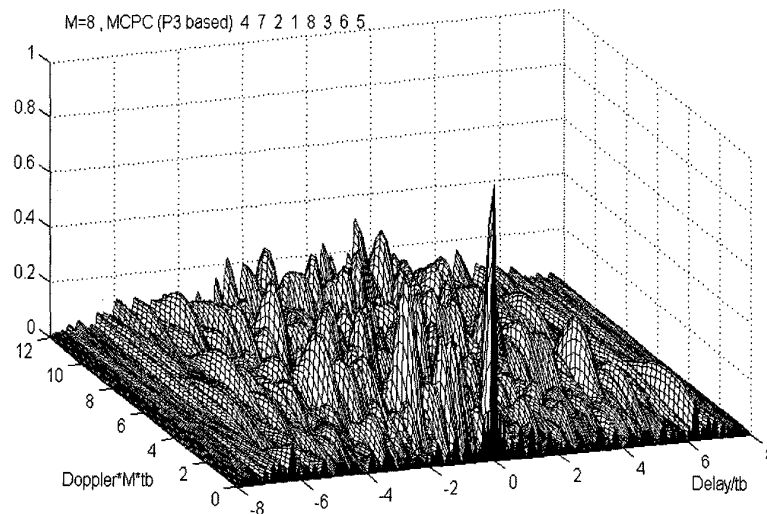


Fig. 5. Ambiguity function of  $8 \times 8$  MCPC pulse (P3 based, no frequency weighting).

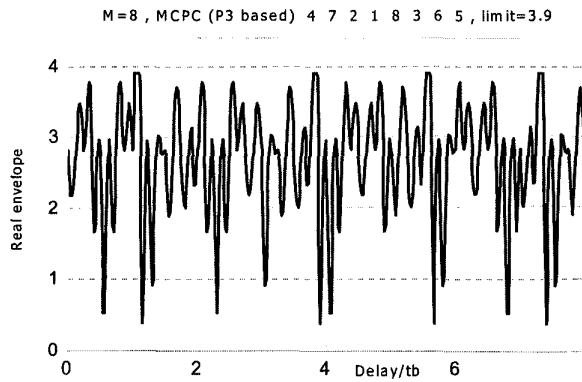


Fig. 6. Real envelope of signal in Fig. 2, after hard limiting.

A P3 or P4 signal will exhibit a sinc-squared shaped power-spectrum with first null at  $1/t_b$ . On the other hand, while each one of the subcarriers of an MCPC signal has a fixed real-amplitude, their sum exhibits a variable real-amplitude, as depicted in Fig. 4. (In Fig. 4, PMEPR = 2.93.)

Finally we observe in Fig. 5 the 1st and 2nd quadrants of the ambiguity function  $|\chi(\tau, \nu)|$  of this particular single MCPC pulse. The thumbtack shape is typical of all MCPC pulses. Recall that the ambiguity function of P3, P4 or linear FM signals exhibits a diagonal ridge.

The variable amplitude of an MCPC signal may require a linear power amplifier (LPA) in the transmitter. In LPA it is important to minimize the PMEPR. Furthermore, the signal peaks may be distorted if the amplifier dynamic range is fully utilized. We found out that limiting the signal peaks, at the transmitter end, degrades the receiver response rather gracefully. This is demonstrated in Fig. 6 in which the signal amplitude is hard-limited yielding PMEPR = 1.95 (compared with PMEPR = 2.93 in Fig. 4) and by the resulting correlation response

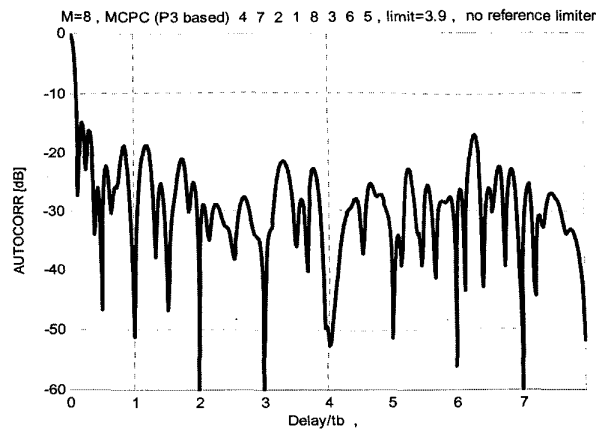


Fig. 7. Crosscorrelation of  $8 \times 8$  MCPC pulse with hard limiting on transmit.

in Fig. 7, which is not much different from the autocorrelation in Fig. 2.

### III. COHERENT TRAIN OF COMPLEMENTARY MCPC PULSES

A train of  $M M \times M$  MCPC pulses can be complementary in time as well as in frequency. (Namely, one sees a complementary set when looking at all the frequencies of a single pulse, as well as when looking at one frequency in all the pulses.) This happens when each pulse in the train is a different one-way cyclic frequency shift of the first pulse. An example of such an arrangement is presented by the array within Fig. 8. A column represents a pulse. The last column indicates that the 8 carriers of the last pulse were modulated according to the same permutation of the rows in Table I, as the single pulse used in Fig. 2. The 7 remaining cyclic shifts of this particular order will be used to create the other 7

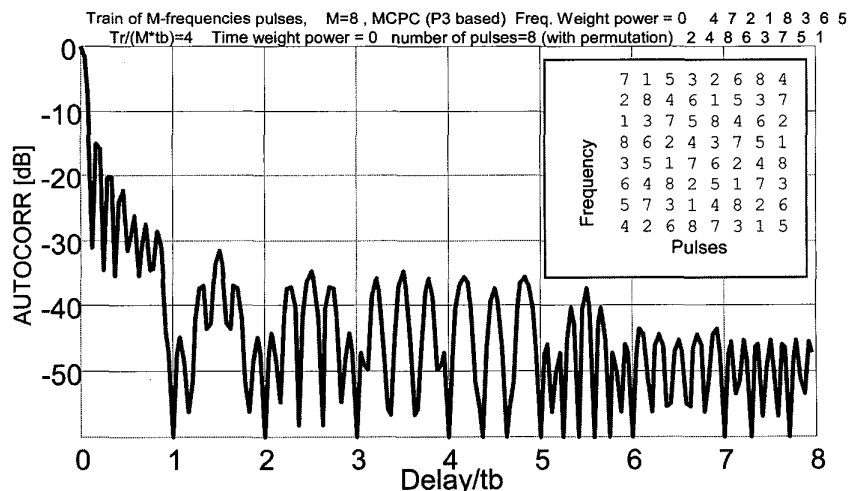


Fig. 8. Autocorrelation of coherent train of 8 complementary MCPC pulses (P3 based, no frequency weighting).

pulses. For example, one cyclic shift upward will be used to generate the first pulse, two shifts created the fifth pulse, and so on. The order (along frequency) of the basic pulse appears in the first row of the heading, and the order (along time) of the pulses appears in the second row. There are  $M!$  different ways to order the basic pulse along frequencies, and for each choice of a basic pulse there are  $M!$  different ways to order the pulses in time.

Comparing Fig. 8 with Fig. 2 demonstrates a significant reduction of the autocorrelation sidelobes. The reduction however applies to  $t_b < |\tau|$ . This should be expected because the autocorrelation of a coherent train of single-frequency pulses, constructed from  $M$  element complementary sequences, will yield zero sidelobes for the delay range  $t_b < |\tau| < Mt_b$ , but not within the first element, namely for  $|\tau| < t_b$ .

The delay axis in Fig. 8 is limited to the duration of a pulse ( $= Mt_b$ ). The autocorrelation within that delay is not affected by the pulse repetition interval  $T_r$  as long as  $T_r$  is larger than twice the pulsewidth, namely  $T_r > 2Mt_b$ . The pulse repetition interval does affect the ambiguity function for non-zero Doppler. The dramatic improvement in sidelobe reduction for  $t_b < |\tau| < Mt_b$  by a train of complementary MCPC pulses, invites a search for a method for sidelobe reduction in the delay range of  $|\tau| < t_b$ . Amplitude weighting of the different frequencies (which we call frequency weighting) is a well-established method for reducing autocorrelation sidelobes in linear FM radar signals [7]. We found out that frequency weighting was not very effective in a *single* MCPC pulse because it yielded meaningful autocorrelation sidelobe reduction only over the limited delay range  $|\tau| < t_b$ , but did not help over the larger remaining delay range of  $t_b < |\tau| < Mt_b$ . Furthermore it eliminated the complete nulls at multiples of  $t_b$ , because with weighting, the  $M \times M$  set was not complementary anymore. However, once we found out that a complementary train of MCPC pulses dramatically reduces sidelobes in that larger delay range  $t_b < |\tau| < Mt_b$ , it became obvious that combining complementary pulse train and frequency weighting can reduce autocorrelation sidelobes over the entire sidelobes delay range  $t_b/M < |\tau| < Mt_b$ . The combination also maintains the complete nulls at multiples of  $t_b$  within that delay range.

In conventional constant-amplitude radar signals, weighting is usually implemented only at the receiver, in order not to lose the constant-amplitude property of the transmitted signal. Weighting on-receive causes a deviation from matched-filter processing and results in some signal-to-noise ratio (SNR) loss. In our case, the signal is of variable amplitude even before adding weights, and special measures (like linear power amplifiers or an array) are already required. Hence, applying different amplitude to each subcarrier (see Fig. 1) adds no difficulty to the one already

encountered. Thus, weighting could be split between the transmitter and the receiver and matched filtering is maintained.

Of the extensive knowledge regarding weighting windows, we limited our numerical trials to only few windows.

- 1) The generalized cosine window described by

$$W_n = \left[ a_0 + a_1 \cos \frac{2\pi(n - \frac{1}{2})}{M} \right]^\alpha, \quad n = 1, \dots, M. \quad (6)$$

Note that setting  $a_0 = 0.53836$ ,  $a_1 = -0.46164$ , and  $\alpha = 0.5$  at both transmitter and receiver obtains sidelobe reduction similar to the reduction achieved by a Hamming window at the receiver end only.

- 2) The Kaiser window

$$W_n = \left[ I_0 \left( \beta \sqrt{1 - \frac{(2n + 2 - N)^2}{N^2}} \right) / I_0(\beta) \right]^\alpha, \quad n = 1, 2, \dots, N. \quad (7)$$

- 3) The Chebyshev family of windows [8].

The weight  $W_n$  now multiplies the signal of the  $n$ th subcarrier as noted in (2). To the  $M = 8$  MCPC complementary pulse train used in Fig. 5, we added weighting according to (6). The resulted magnitude of the ACF is plotted in Fig. 9. Comparing Figs. 8 and 9 demonstrates the sidelobe reduction due to frequency weighting.

The ambiguity function of a complementary train of  $M$  MCPC pulses, with or without weighting, depends on the pulse repetition interval  $T_r$ . The partial *periodic* ambiguity function plotted in Fig. 10 was obtained for an arbitrary case in which the pulse interval was 4 times the MCPC pulse duration, namely  $T_r = 4Mt_b$  and the weighting was according to (6). Because of the periodicity in time, the response in Doppler exhibits peaks at multiples of  $\nu = 1/T_r = 0.25/Mt_b$ , the first of which is seen in Fig. 10. However, since the pulses in the train are different from each other there are no pronounced recurrent peaks at multiples of  $T_r$ . For comparison, Fig. 11 presents partial *periodic* ambiguity function of a coherent train of 8 identical, single-frequency P4 pulses, with the same pulsewidth as the MCPC pulses. In order to obtain a similar bandwidth the P4 pulse was constructed from  $M = 64$  elements and included intrapulse weighting. The zero-Doppler cuts of Figs. 10 and 11 appear in Fig. 12. Note in Fig. 12 that thanks to the similar bandwidth, both signals exhibit a similar ACF mainlobe. The P4 signal exhibits strong recurrent lobes at multiples of  $T_r$ , but the sidelobe strips around them are much lower than the corresponding sidelobes of the MCPC. The constant volume property of the ambiguity function

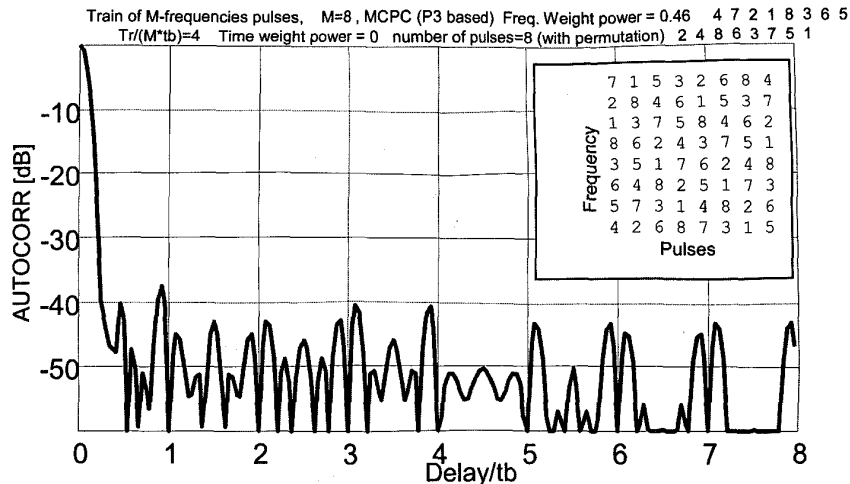


Fig. 9. Autocorrelation of coherent train of 8 complementary MCPC pulses (P3 based, with frequency weighting).

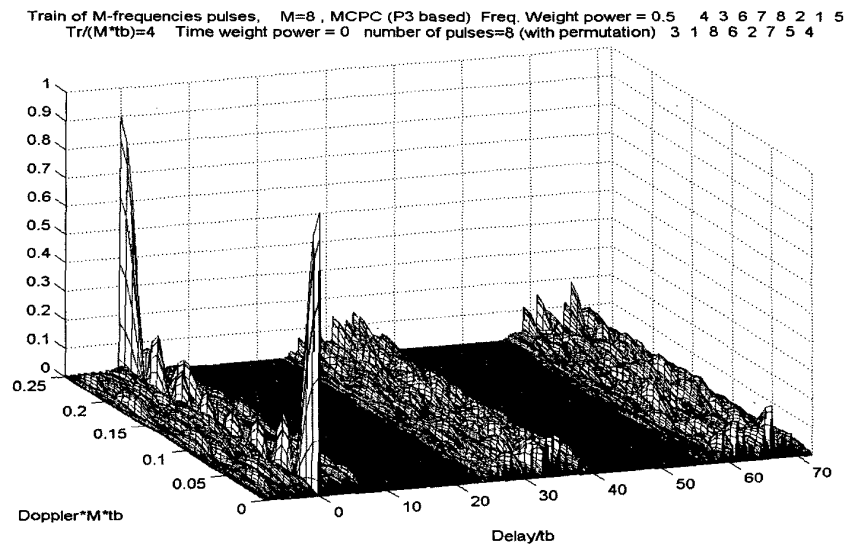


Fig. 10. Partial periodic ambiguity function of 8 diverse  $8 \times 8$  MCPC pulses (P3 based, with frequency weighting).

is maintained by shifting volume from the additional peaks (in P4) to the strips around them (in MCPC).

The *periodic* ambiguity function [9, 10], describes the response of the receiver when the received signal contains many more pulses (or periods) than the  $M$  pulses to which the receiver is matched. The real envelopes of the transmitted and reference signals yielding Figs. 10 and 11, are described in Fig. 13.

There have been attempts to reduce the recurrent lobes in linear FM pulse train by introducing chirp rate diversity from pulse to pulse [11]. However, the reduction reported for chirp diverse linear FM pulse train, was nowhere as pronounced as the reduction demonstrated in Fig. 10 for MCPC pulse train.

The favorable ambiguity function properties, caused by complementarity in each pulse as well as in each frequency, require that the number of diverse

pulses in the coherent train should equal the number of frequencies. It turns out that the ACF mainlobe compression can be doubled without increasing the number of pulses. This can be achieved by doubling the number of carriers. In each pulse the  $M \times M$  array that modulated carriers 1 to  $M$ , will also modulate carriers  $M + 1$  to  $2M$ . This idea does not stop at doubling. It can be extended to tripling, quadrupling, etc.

#### IV. MCPC BASED ON 2-VALUED COMPLEMENTARY SET

The P4 phase coded sequences used so far to construct the MCPC complementary set are polyphase code sequences. There are 2-valued phase sequences that also exhibit ideal periodic autocorrelation, and

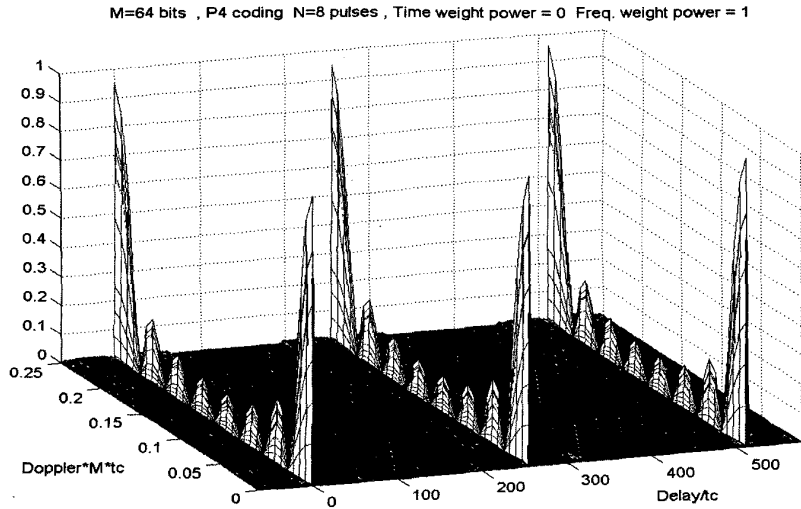


Fig. 11. Partial periodic ambiguity function of 8 identical P4 pulses.

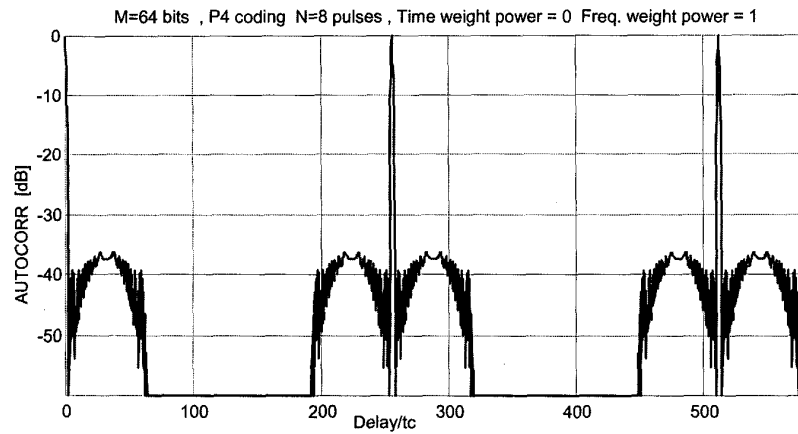
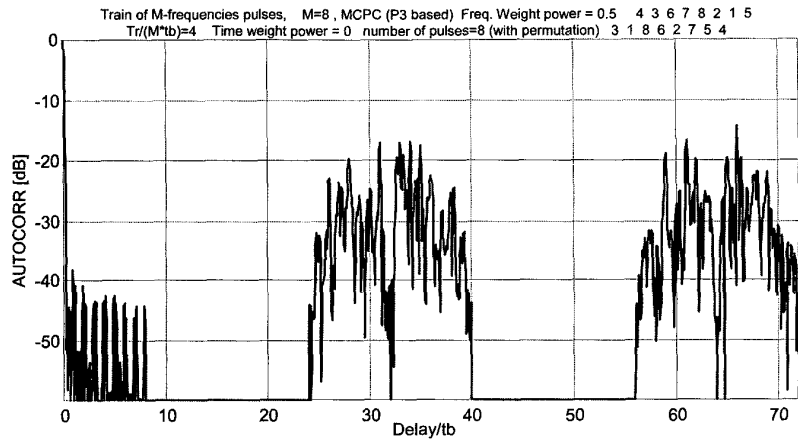


Fig. 12. Partial autocorrelation in dB of train of MCPC (top) and P4 (bottom) pulses (i.e., zero-Doppler cuts of Figs. 10 and 11).

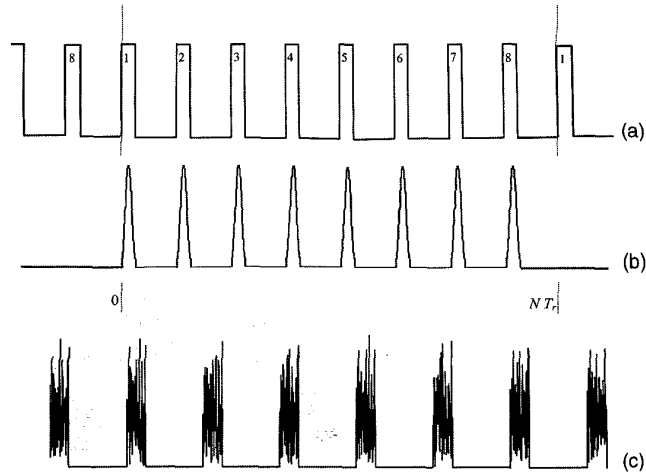


Fig. 13. Real envelopes. (a) Transmitted P4 pulses. (b) Reference P4 pulses with intrapulse (frequency) weighting. (c) Transmitted (and also reference) diverse  $8 \times 8$  MCPC pulses with intrapulse (frequency) weighting.

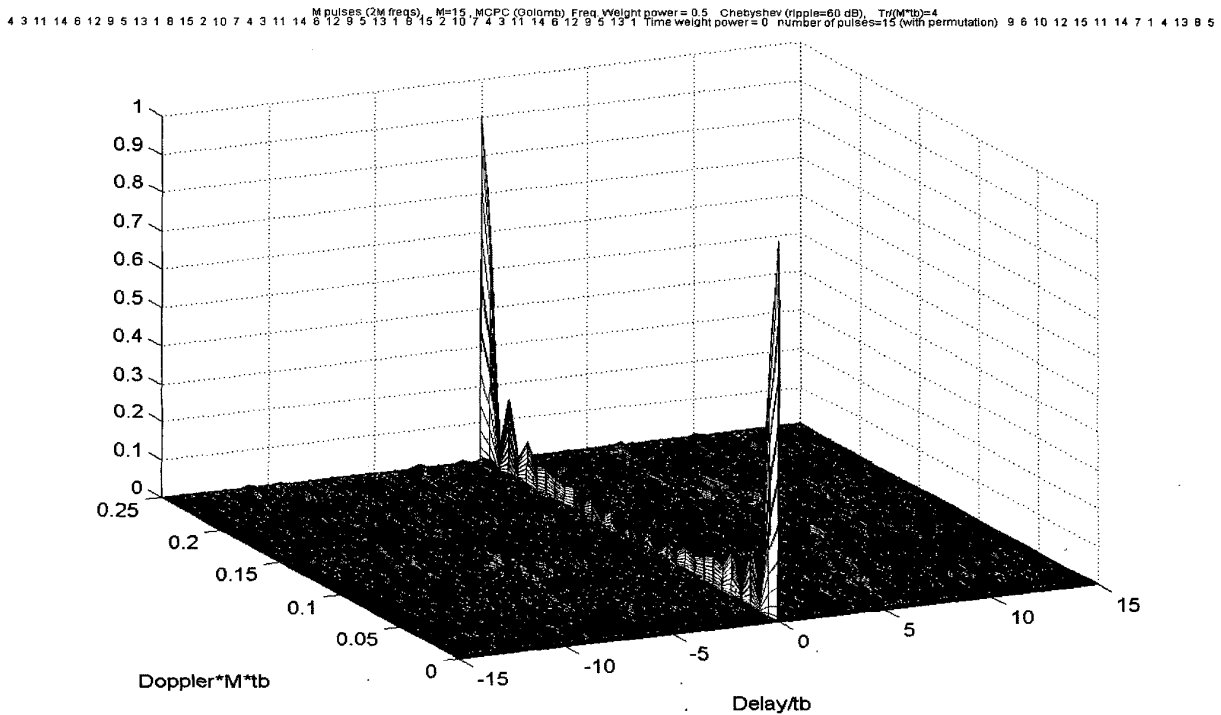


Fig. 14. Partial ambiguity function of train of fifteen  $45 \times 15$  MCPC pulses (Golomb based) with Chebyshev frequency weighting.

can serve to construct a complementary set and an MCPC signal. Such alternatives are the sequences described by Golomb [6]. A simple example is based on a Barker code of length 7 [ $+++-+--$ ], in which the two phase values are not 0 and  $180^\circ$  but 0 and  $138.59^\circ (= \arccos(-3/4))$ . Golomb codes exist for lengths 3, 7, 11, 15, 19, 23, 31, 35, 43, 47, 59, ... Fig. 14 displays the partial ( $-Mt_b < \tau < Mt_b$ ) periodic ambiguity function of a coherent train of  $M = 15$  diverse MCPC pulses based on a 15-element Golomb

code. The number of carriers  $N$  was 45, using the concept discussed in the previous paragraph. Intrapulse frequency weighting is used (Chebyshev,  $-60$  dB), but no interpulse weighting. Fig. 15 presents the partial periodic autocorrelation up to and including the third bit out of 15 bit in the pulse ( $0 < \tau < 3t_b$ ). The compression ratio without frequency weighting should have been  $N \times M = 45 \times 15 = 675$ . With frequency weighting we observe compression ratio of about 420.

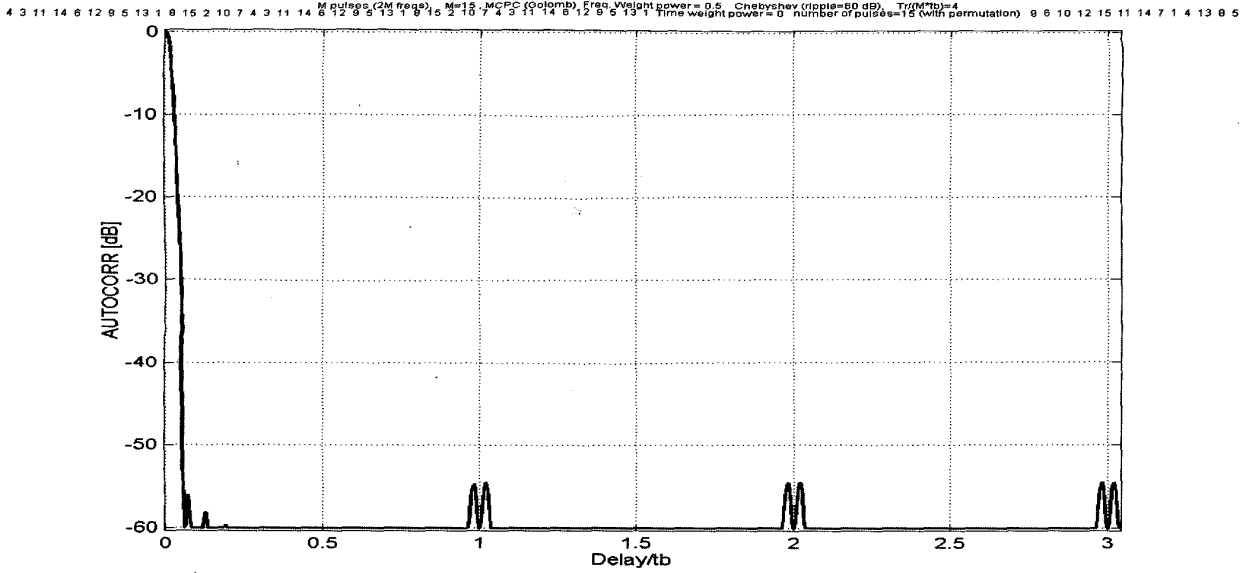


Fig. 15. Partial ACF of train of fifteen  $45 \times 15$  MCPC pulses (Golomb based) with Chebyshev frequency weighting.

## V. CW MODE

In CW radar applications, the “matched-filter” delay response is determined by the periodic ACF. Here a single-carrier signal, like P4, has an advantage since its periodic ACF is ideal by definition, while an MCPC signal does not have an ideal periodic ACF. However, we suggest ways to generate MCPC periodic signals with near-ideal periodic ACF.

Each one of the many *identical* periods of a periodic MCPC signal is a *single* multicarrier pulse. In other words, the CW signal is constructed from contiguous, identical, multicarrier pulses. The multicarrier pulse (now called period) is based, as before, on a basic code sequence, which, by itself, exhibits ideal periodic ACF. The definition of a single-pulse signal given in (2) and (3) now describes one period of the CW signal. The  $N$  sequences modulating the  $N$  carriers are all cyclic shifts of the basic ideal code sequence. However, the  $N$  sequences do not have to constitute a complementary set. Removing this requirement allows repeating the same sequence at several carriers. Also, the number of carriers  $N$  need not be equal to the number of elements  $M$  in the basic sequence. There is however one restriction on the relationship between  $N$  and  $M$ —the product  $M(N + 1)$  must be even.

If that restriction is met and if the basic code sequence exhibits ideal periodic ACF, then it can be proved that the periodic ACF of the multicarrier periodic signal is *independent of the type of the basic sequence*, and it becomes a function only of  $M$ ,  $N$ , the weights  $W_n$ , and the shifts  $\theta_n$  (dimensionless integer), where  $n = 1, 2, \dots, N$ .  $\theta_n$  tells us by how many elements was the sequence on the  $n$ th carrier shifted

relative to the basic sequence. That universal periodic ACF is given by

$$R(\tau_b + \eta) = (-1)^{(N+1)\tau} \sum_{n=1}^N \sum_{l=1}^N W_n W_l^* \times \exp \left[ 2\pi j \left( l - \frac{N+1}{2} \right) \frac{\eta}{t_b} \right] \times [I_1 \delta([\theta_n - \theta_l + i + 1]_M) + I_2 \delta([\theta_n - \theta_l + i]_M)] \quad (8)$$

where  $\delta$  implies Kronecker delta,  $[\theta]_M$  implies  $\theta$  modulo  $M$ ,

$$0 \leq \eta < t_b \quad (9)$$

$$I_1 = \begin{cases} \eta, & \text{when } n = l \\ \eta \frac{\sin \beta}{\beta} \exp(j\beta), & \text{when } n \neq l \end{cases}, \quad \beta = \pi(n-l) \frac{\eta}{t_b} \quad (10)$$

$$I_2 = \begin{cases} t_b - \eta, & \text{when } n = l \\ -I_1, & \text{when } n \neq l \end{cases} \quad (11)$$

The universal expression in (8) led to some interesting designs of CW MCPC signals. The first one uses consecutive shifts, namely

$$\theta_n = n, \quad n = 1, 2, \dots, N. \quad (12)$$

With this choice of shifts, and when  $N < M/2$ , the periodic ACF exhibits zero sidelobes over the delay range  $Nt_b < \tau < (M - N)t_b$ . When  $M$  is odd, the central periodic ACF bit is always sidelobe-free. Fig. 16 presents three examples of the periodic ACF for this signal (consecutive shifts) and for the cases of  $M = 15$ , and three different number of frequencies,  $N = 5, 10$ , and  $25$ . Fig. 16 demonstrates that as  $N$

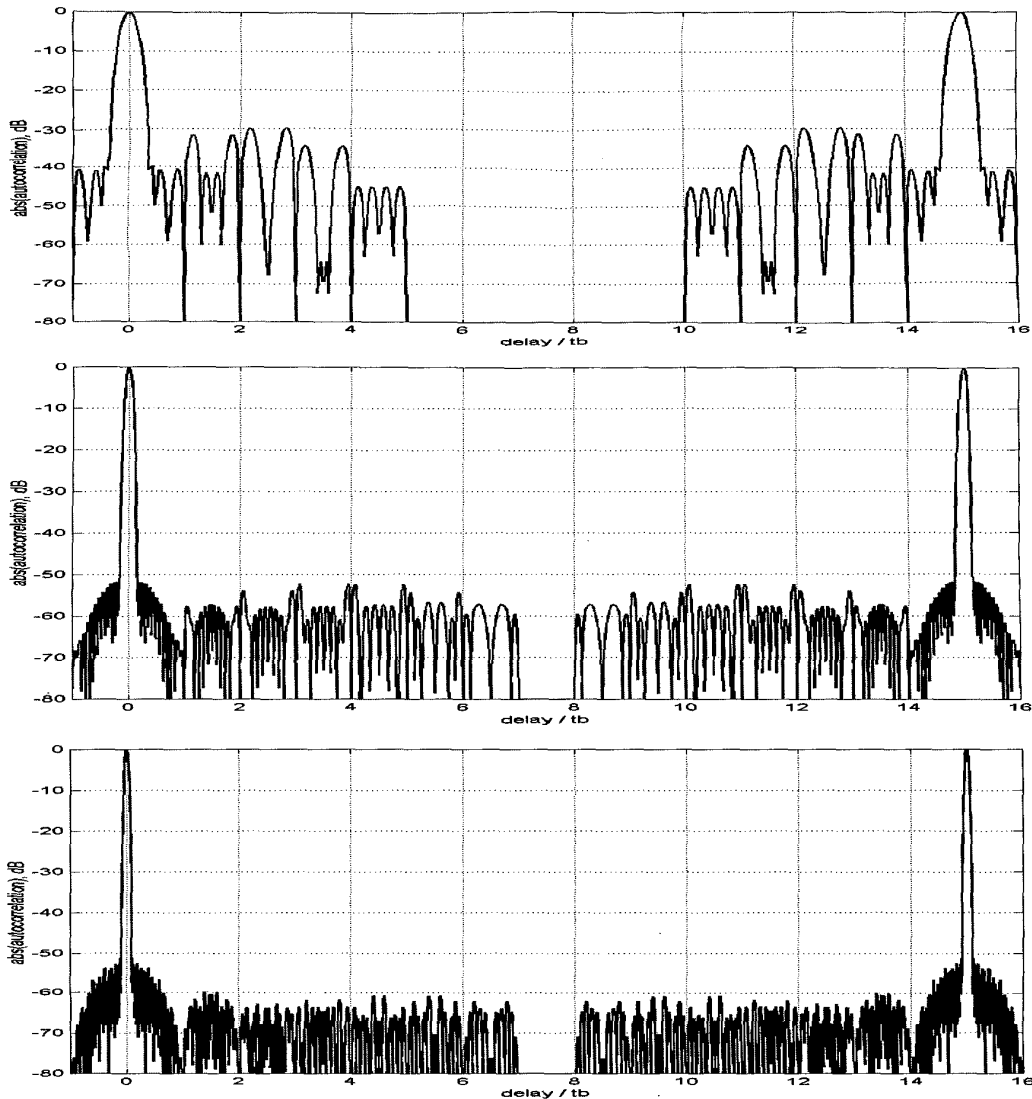


Fig. 16. Partial ACF of MCPC signal with  $N$  frequencies, based on consecutive cyclic shifts of any ideal sequence of length  $M = 15$ . Frequency weighting: Chebyshev  $-54$  dB.  $N = 5$  (top), 15 (middle), 25 (bottom).

increases the sidelobe level and the mainlobe width decreases. The frequency weighting for this design was according to a Chebyshev window.

In the second design there are no shifts at all. The same code sequence modulates all the subcarriers, i.e.,  $\theta_n = 1, n = 1, 2, \dots, N$ . With this choice of (no) shifts, the periodic ACF exhibits zero sidelobes over the delay range  $t_b < \tau < (M - 1)t_b$ , namely, everywhere except the first and last code element (bit). In order to reduce the PACF sidelobes in the remaining first and last bit, it turns out that the polarity of the weights should *alternate* between consecutive carriers. Finally, the frequency weighting for this design was the Kaiser window. Fig. 17 presents three examples of the periodic ACF for this signal, for the case of  $M = 15$ , and for three different number of frequencies,  $N = 5$ ,

10, and 25. Fig. 17 demonstrates that indeed there are no sidelobes outside the first and last bit, and as before, as  $N$  increases the sidelobe level and the mainlobe width decrease.

Based only on the periodic ACF (Figs. 16 and 17), clearly the second design is better. However we still need to check the periodic ambiguity function and the real amplitude of the signal. To obtain the periodic ambiguity function we must first define the type of code, the number of periods  $P$  coherently processed by the receiver, and the interperiod weighting on receive (which affects Doppler sidelobes). The meaning of  $P$  and of the interperiod weighting are demonstrated in Fig. 18. The top row represents the transmitted periodic signal where each period is the same  $N \times M$  multicarrier pulse. The second

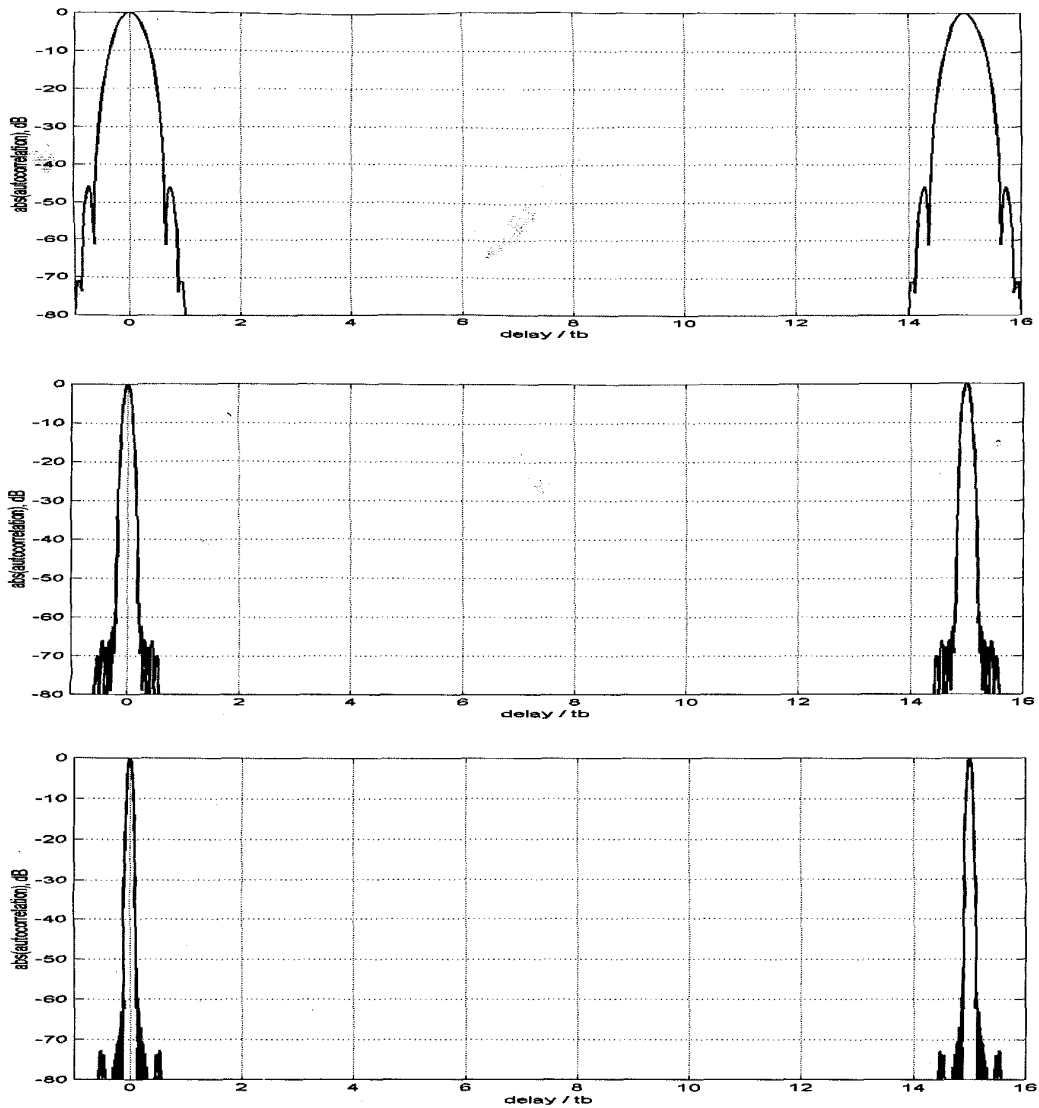


Fig. 17. Periodic ACF of MCPC signal with  $N$  frequencies, based on any ideal sequence of length  $M = 15$ . No cyclic shifts. Alternating polarity. Kaiser weighting.  $N = 5$  (top), 15 (middle), 25 (bottom).

row describes a reference signal at the receiver that extends over  $P$  periods, with no weighting. In the third row, smooth interpulse weighting multiplies the receiver reference signal. Such smooth weighting is optimal as far as reducing Doppler sidelobes. However implementing filters matched to non-zero Doppler is more difficult. In the last row the smooth weighting window was replaced by a stepwise window, which allows simpler implementation of Doppler filters. Finally the periodic ambiguity function depends also on the type of code. Golomb code sequence was the basis for the  $15 \times 15$  MCPC signal whose partial periodic ambiguity function is plotted in Fig. 19. The design was based on consecutive cyclic shifts (defined in (12)). The number of periods processed coherently was eight, and smooth Hamming on-receive interpulse

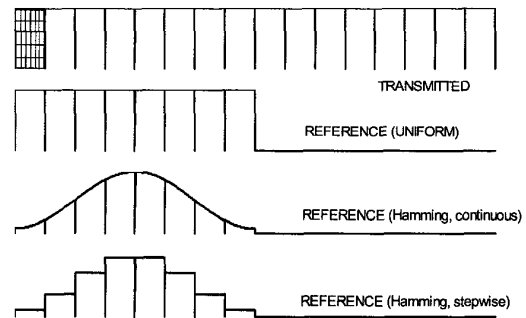


Fig. 18. Coherent matched processing of  $P$  periods of a CW signal, with and without interpulse weighting on receive.

CW signal, M=15, MCPC (Golomb) 0 and 151.045 deg., 8 periods, T. Wt (cont.) power = 1 Fr. Wt. power = 0.5  
 Freq. order = 1 2 3 4 5 6 7 8 9 10 11 12 13 14 15

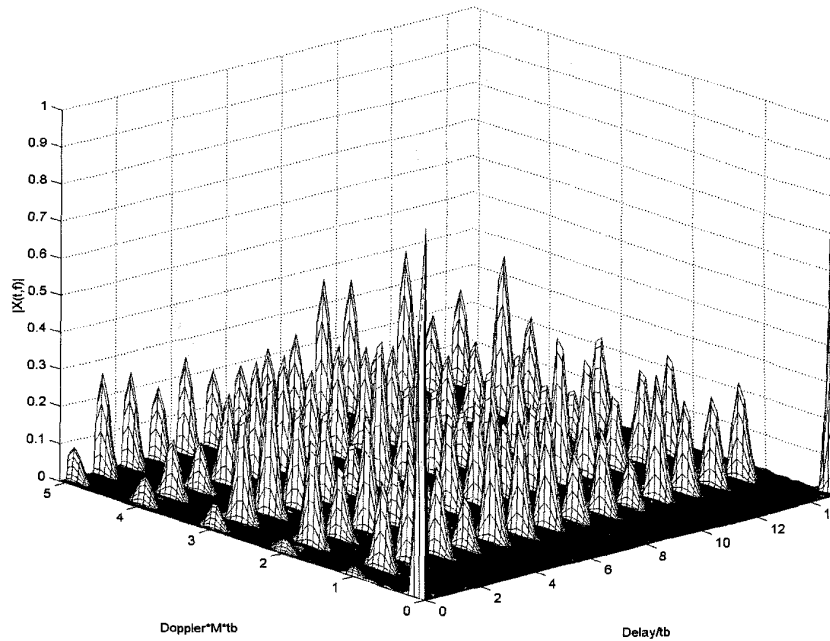


Fig. 19. Delay-Doppler response of 8 period processing of periodic CW signal. Each period consists of frequency weighted  $15 \times 15$  MCPC pulse (Golomb based). Smooth interperiod weighting used on receive.

window was used. The frequency weighting, performed at both transmit and receive was the square root of Hamming. The periodic ambiguity function in Fig. 19 yields practically no sidelobes over the Doppler range of  $-1/Mt_b < \nu < 1/Mt_b$  that can be observed with a linear vertical scale. If we had used the second design (no cyclic shifts) with the same parameters, the difference between the two periodic ambiguity functions could hardly be observed due to the linear vertical scale.

The major difference between the two designs becomes apparent when we look at the real envelope of the two signals (Fig. 20). The first design (in which the code modulating a given carrier is shifted by one element relative to the code modulating the previous carrier) yields a typical MCPC variable envelope, with a tolerable PMEPR (top part of Fig. 20). The second design yields narrow pulses, spaced  $t_b$  apart, each with a width of about  $t_b/N$ . The phase during each pulse is practically constant, and the 15 phases of the 15 elements in each period, are equal to the phases of a Golomb sequence of length 15. This second design resembles known methods for generating impulses using Poisson summation formula. The resulted real envelope (bottom part of Fig. 20) looks like a train of impulses. This kind of envelope does not suit an LPA. Instead it calls for transmitter implementation based on feeding each one of the carriers to a different array element, with power combining in the air. More on this subject in the following section devoted to implementation issues.

These CW signals are only two examples out of many possible ones. For every choice of code length  $M$  and number of subcarriers  $N$ , there are additional parameters that can be changed. e.g., the maximum code shift allowed ( $\max \theta_n$ ), the code shifts order along the  $N$  frequencies, and the  $N$  complex weights. Among the parameters to optimize are the PMEPR of the real envelope and the periodic ACF mainlobe-width and sidelobe level.

## VI. BRIEF DISCUSSION OF IMPLEMENTATION ISSUES

On the transmitter side, two implementation approaches seem viable. In low-power radar systems, where the output power is within the power limits of LPAs, a recommended approach would be to generate the complex envelope of the MCPC signal as one entity. Modulate it on a central carrier and amplify it using LPA. A method for generating the complex envelope using fast Fourier transform (FFT) was first suggested in [12] and is the preferred approach in OFDM communications and broadcasting transmitters [13]. In high power radar systems, a possible approach would be to generate each carrier separately, while maintaining coherency, relative phase, and relative amplitude, and feed each carrier to a different antenna array element. Power combining will take place in the air.

The receiver end will not be affected by the method used in the transmitter. After converting

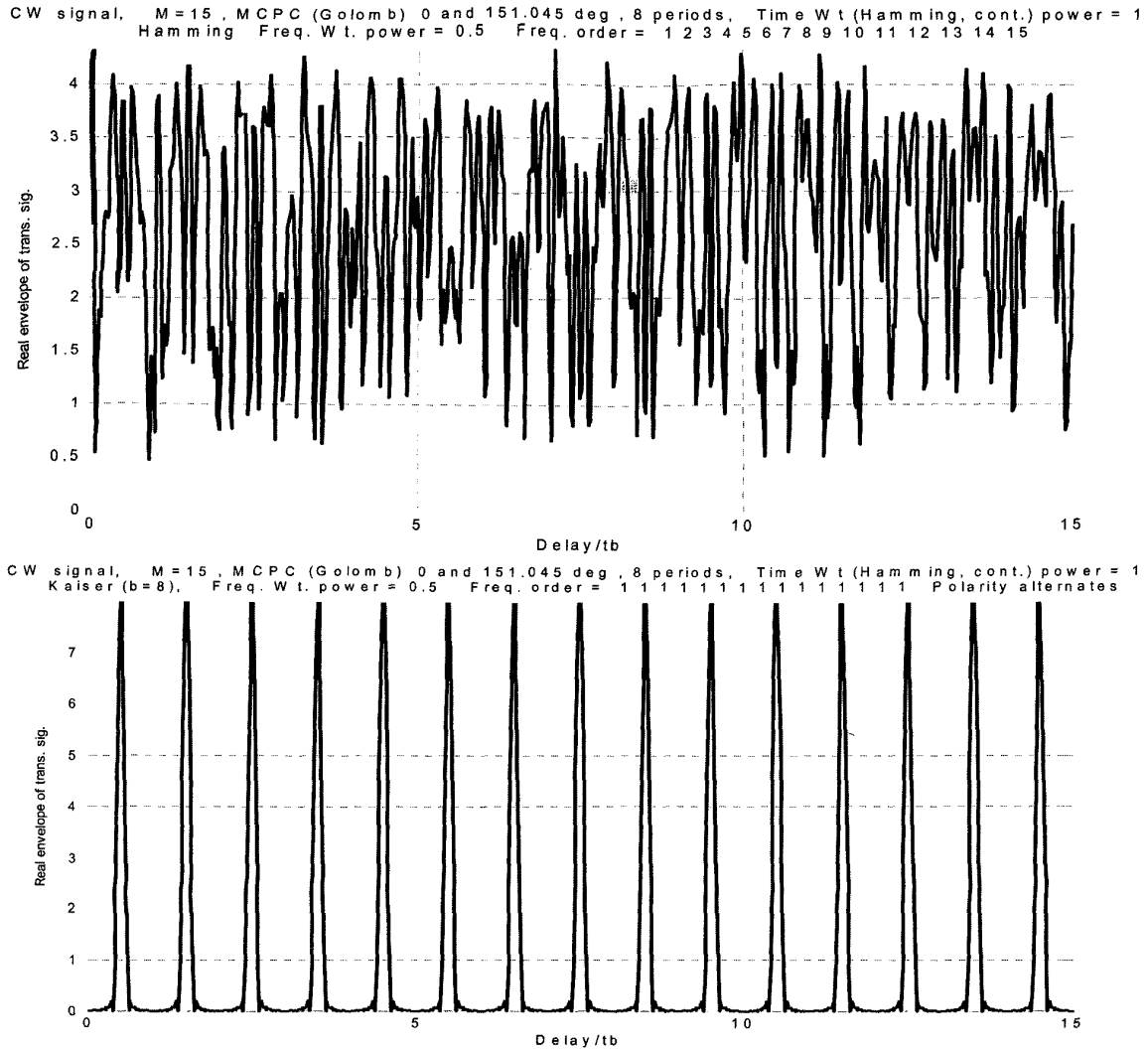


Fig. 20. Real envelope of two frequency-weighted, multicarrier CW signals using 15 subcarriers. Top: using consecutive cyclic shifts of 15-element Golomb code sequence. Bottom: using identical 15-element Golomb code sequence on all 15 subcarriers, with alternating polarity.

the signal back to baseband and recovering the complex envelope, an inverse FFT will separate the subcarriers and recover the  $N$  sequences modulated on the  $N$  carriers. Digital crosscorrelation can then be performed between each one of the  $N$  received sequences and the corresponding one of  $N$  reference sequences (with their respective weighted magnitude). The crosscorrelation complex outputs are then combined to yield the postcompression output. In a coherent pulse train system ( $M$  pulses) the postcompression complex outputs from the  $M$  pulses can either be coherently added to yield a zero-Doppler matched filter output, or fed to an  $M$  input FFT, yielding  $M$  different Doppler outputs. Interpulse weighting on-receive could be implemented by multiplying the  $M$  inputs to the FFT by the  $M$  weights.

A special case was the CW MCPC signal based on no cyclic shifts. The sum of  $N$  fixed-amplitude carriers resulted an overall transmitted signal, in which each element of duration  $t_b$  was reduced to a much narrower pulse of a single carrier with interpulse phase coding. Transmitting such a signal could be implemented by either using an array approach, or by transmitting single-frequency, phase-coded narrow pulses. In either case the matched filter in the receiver could be implemented simply by crosscorrelation with a baseband train of narrow pulses, with matching phase coding.

## VII. CONCLUSIONS

A coherent train of  $M$  diverse  $M \times M$  MCPC pulses was compared with a coherent train of  $M$

identical pulse-compression pulses (e.g., P4), each constructed from  $K$  chips. If the total pulse duration is identical and  $K = M^2$ , the bandwidth is comparable and the same pulse compression ratio is achieved. The ambiguity functions, however, differ dramatically.

As is well known, the ambiguity function of a coherent train of identical pulse-compression pulses exhibits the typical “bed of nails” shape with recurrent lobes in delay and Doppler. With proper interpulse and intrapulse weighting, the sidelobe pedestal strips can be made very low. In other words, the volume of the ambiguity function is concentrated in the recurrent lobes and not in the sidelobe pedestal strips.

The opposite occurs in the ambiguity function of a coherent train of  $M$  diverse  $M \times M$  MCPC pulses. There are no recurrent lobes in delay (only in Doppler at zero-delay), and the volume is diverted to raise the sidelobe pedestal strips. We can conclude that MCPC pulses in a coherent pulse train can provide an alternative to single-frequency signals, when recurrent lobes pose a bigger problem than the sidelobe pedestal.

In CW mode (contiguous identical pulses) a multicarrier signal can be designed whose periodic ACF exhibits narrow mainlobe, with width equal to the code element (chip) duration divided by the number of carrier frequencies. The sidelobe spread in delay can be limited to any desired number of chips by controlling the cyclic shifts between the code sequences modulating the different subcarriers. A universal expression of the periodic ACF was given, which is independent of the type of ideal sequence used to construct the signal.

Finally we point out that a single  $M \times M$  MCPC pulse, based on one given sequence, can be designed in  $M!$  different permutations. A train of  $M$  diverse pulses can be constructed in  $(M!)^2$  different permutations. The cross ambiguity between different permutations is a flat, low pedestal, with no major lobes. This implies good immunity against mutual interference or jamming.

NADAV LEVANON  
 ELI MOZESON  
 Dept. of Electrical Engineering-Systems  
 Tel Aviv University  
 P.O. Box 39040  
 Tel Aviv 69978  
 Israel  
 E-mail: (nadav@eng.tau.ac.il)

#### REFERENCES

- [1] Levanon, N. (2000)  
 Multifrequency radar signals.  
 In *Proceedings of the IEEE International Radar Conference*, Alexandria, VA, May 2000, 683–688.
- [2] Levanon, N. (2000)  
 Multifrequency complementary phase-coded radar signal.  
*IEE Proceedings—Radar, Sonar and Navigation*, **147**, 6 (Dec. 2000), 276–284.

- [3] Tseng, C. C., and Liu, C. L. (1972)  
 Complementary sets of sequences.  
*IEEE Transactions on Information Theory*, **IT-18**, 5 (Sep. 1972), 644–652.
- [4] Popovic, B. M. (1990)  
 Complementary sets based on sequences with ideal periodic autocorrelation.  
*Electronics Letters*, **26**, 18 (Aug. 1990), 1428–1430.
- [5] Lewis, B. L., Kretschmer, F. F., and Shelton W. W. (1986)  
*Aspects of Radar Signal Processing*.  
 Norwood, MA, Artech House, 1986.
- [6] Golomb, S. W. (1992)  
 Two-valued sequences with perfect periodic autocorrelation.  
*IEEE Transactions on Aerospace and Electronic Systems*, **28**, 2 (Apr. 1992), 383–386.
- [7] Farnet, E. C., and Stevens, G. H. (1990)  
 Pulse compression radar.  
 In M. I. Skolnik (Ed.), *Radar Handbook* (2nd ed.).  
 New York: McGraw-Hill, 1990, ch. 10.
- [8] IEEE (1979)  
*Programs for Digital Signal Processing*.  
 New York: Wiley, 1979.
- [9] Freedman, A., and Levanon, N. (1994)  
 Properties of the periodic ambiguity function.  
*IEEE Transactions on Aerospace and Electronic Systems*, **30**, 3 (July 1994), 938–941.
- [10] Getz, B., and Levanon, N. (1995)  
 Weight effects on the periodic ambiguity function.  
*IEEE Transactions on Aerospace and Electronic Systems*, **31**, 1 (Jan. 1995), 182–193.
- [11] Vannicola, V. C., Hale, T. B., Wicks, M. C., and Antonik, P. (2000)  
 Ambiguity function analysis for the chirp diverse waveform (CDW).  
 In *Proceedings of the IEEE International Radar Conference*, Alexandria, VA, May 2000, 666–671.
- [12] Weinstein, S. B., and Ebert, P. M. (1971)  
 Data transmission by frequency-division multiplexing using the discrete Fourier transform.  
*IEEE Transactions on Communications Technology*, **COM-19**, 5 (Oct. 1971), 628–634.
- [13] Rohling, H., May, T., Bruninghouse, K., and Grunheid, R. (1999)  
 Broad-band OFDM radio transmission for multimedia applications.  
*Proceedings of the IEEE*, **87**, 10 (Oct. 1999), 1778–1789.